RECENT SASE FREE ELECTRON LASER RESULTS

J. Rossbach, DESY, Notkestrasse 85, 22603 Hamburg, Germany

Abstract

   The principle of Self-Amplified Spontaneous Emission (SASE) is presently the most promising concept to extend the working principle of Free Electron Lasers (FEL) to the VUV and X-ray wavelength regime. Several laboratories (e.g. SLAC, ANL, DESY, Spring8) are considering large-scale installations which may be regarded as truly fourth-generation light sources, providing full transverse coherence and brilliance performance many orders of magnitude above present-day synchrotron radiation sources. The paper discusses key accelerator physics challenges to be met for achieving SASE FEL gain and power saturation as well as recent SASE demonstration experiments pursued at Los Alamos (LANL/UCLA), Argonne (LEUTL) and DESY (TTF FEL

1 INTRODUCTION

   X-ray lasers are expected to open up new and exciting areas of basic and applied research in biology, chemistry and physics. Due to recent progress in accelerator technology the attainment of the long sought-after goal of wide-range tunable laser radiation in the Vacuum-Ultraviolet and X-ray spectral regions is coming close to realization with the construction of Free-Electron Lasers (FEL) based on the principle of Self-Amplified Spontaneous Emission (SASE). In a SASE FEL lasing occurs in a single pass of a relativistic, high-quality electron bunch through a long undulator magnet structure.

   The photon wavelength λ_{ph} of the first harmonic of FEL radiation is related to the period length λ_u of a planar undulator by

$$\lambda_{ph} = \frac{\lambda_u}{2\gamma^2}\left(1 + \frac{K^2}{2}\right) \qquad (1)$$

where $\gamma = E/m_e c^2$ is the relativistic factor of the electrons, $K = eB_u\lambda_u/2\pi m_e c$ the 'undulator parameter' and B_u the peak magnetic field in the undulator. Equation (1) exhibits two main advantages of the free-electron laser: the free tunability of the wavelength by changing the electron energy and the possibility to achieve very short photon wavelengths.

   For most FELs [1] presently in operation [2], the electron beam quality and the undulator length result in a gain of only a few percent per undulator passage, so that an optical cavity resonator and a synchronized multi-bunch electron beam have to be used. At very short wavelengths, normal-incidence mirrors of high reflectivity are unavailable. Therefore the generation of an electron beam of extremely high quality in terms of emittance, peak current and energy spread, and a high-precision undulator of sufficient length are essential. Provided the spontaneous radiation from the first part of the undulator overlaps the electron beam, the electromagnetic radiation interacts with the electron bunch leading to a density modulation (micro-bunching) which enhances the power and coherence of radiation. In this "high gain mode" [3,4,5], the radiation power $P(z)$ grows exponentially with the distance z along the undulator

$$P(z) = P_0 \cdot A \cdot \exp(2z/L_g), \qquad (2)$$

where L_g is the field gain length, P_0 the effective input power (see below), and A the input coupling factor [4,5]. A is equal to 1/9 in one-dimensional FEL theory with an ideal electron beam.

Since the desired wavelength is very short, there is no laser tunable over a wide range to provide the input power P_0. Instead, the spontaneous undulator radiation from the first part of the undulator is used as an input signal to the downstream part. FELs based on this Self-Amplified-Spontaneous-Emission (SASE) principle [6,7] are presently considered the most attractive candidates for delivering extremely brilliant, coherent light with wavelength in the Ångström regime [8-12]. Compared to state-of-the-art synchrotron radiation sources, one expects full transverse coherence, larger average brilliance and, in particular, up to eight or more orders of magnitude larger peak brilliance at pulse lengths of about 200 fs FWHM. Within the last two years, three important proof-of-principle experiments have successfully demonstrated large SASE gain at shorter and shorter wavelength: 12 μm wavelength was achieved 1998 at Los Alamos (here referred to as UCLA/LANL) [13], 530 nm wavelength was achieved 1999 at Argonne (LEUTL) [14], and 109 nm wavelength was achieved 2000 at DESY (TTF FEL)[15]. It is essential that these experiments have been performed at different laboratories and with quite different set-ups. This indicates that the theory to understand and the technology to construct a SASE FEL have attained a rather mature level.

2 EXPERIMENTAL SET-UP

This paper focuses on the description of the FEL at the TESLA Test Facility (TTF FEL) [16] at the Deutsches Elektronen-Synchrotron DESY which is, operating between 80 and 180 nm, to date the FEL with the shortest wavelength. The layout of this machine is shown in Fig. 1.

With respect to the key accelerator components, this layout is, however, representative for all three SASE experiments: They all use a low emittance, photocathode rf electron gun, a linear accelerator based on high-gradient rf cavities and a long, permanent magnet undulator. The TESLA (TeV-Energy Superconducting Linear Accelerator) collaboration consists of 39 institutes from 9 countries and aims at the construction of a 500 GeV (center-of-mass) e+/e- linear collider with an integrated X-ray laser facility [10]. Major hardware contributions to TTF have come from Germany, France, Italy, and the USA. The goal of the TTF FEL is to demonstrate SASE FEL emission in the VUV and, in a second phase, to build a soft X-ray user facility [17,18]. The main parameters for FEL operation are compiled in Table 1.

_____

TTF FEL 1
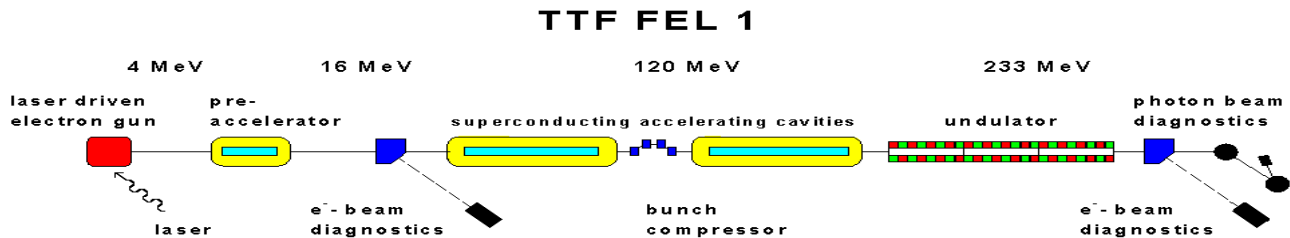
Figure 1: Schematic layout of phase 1 of the SASE FEL at the TESLA Test Facility at DESY, Hamburg. The linac contains two 12.2 m long cryogenic modules each equipped with eight 9-cell superconducting accelerating cavities [21]. The total length is 100 m.

The injector for the TTF FEL is based on a laser-driven 1½-cell rf gun electron source operating at 1.3 GHz [19]. A Cs_2Te cathode [20] is illuminated by a train of UV laser pulses generated in an mode-locked solid-state laser system [21] synchronized with the rf. An energy of up to 50 μJ with a pulse-to-pulse variation of 2 % (rms) is achieved [21]. The UV pulse length measured with a streak camera is $\sigma_t = 7.1 \pm 0.6$ ps . The gun section is followed by a 9-cell superconducting cavity, boosting the energy to 16 MeV. The superconducting accelerator structure has been described elsewhere [22].

The undulator is a fixed 12 mm gap permanent magnet device using a combined function magnet design [23] with a period length of $\lambda_u = 27.3$ mm and a peak field of $B_u = 0.46$ T, resulting in an undulator parameter of K=1.17. The beam pipe diameter in the undulator (9.5 mm) [24] is much larger than the beam diameter (300 μm). Integrated quadrupole structures produce a gradient of 12 T/m superimposed on the periodic undulator field in order to focus the electron beam along the undulator. The undulator system is subdivided into three segments, each 4.5 m long and containing 10 quadrupole sections to build up 5 full focusing-defocusing (FODO) cells. The FODO lattice periodicity runs smoothly from segment to segment. There is a spacing of 0.3 m between adjacent segments for diagnostics. The total length of the system is 14.1 m.

For optimum overlap between the electron and light beams, high precision on the magnetic fields and mechanical alignment are required. The beam orbit straightness in the undulator is determined by the alignment precision of the superimposed permanent-magnet quadrupole fields which is better than 50 μm in both vertical and horizontal direction [25].

Different techniques have been used to measure the emittance of the electron beam [26] and yield values for the normalized emittance of (4 ± 1) π mrad mm for a bunch charge of 1 nC at the exit of the injector. The emittance in the undulator, as determined from quadrupole scans and from a system of wire scanners was typically between 6 and 10 π mrad mm (in both horizontal and vertical phase space). It should be noted that the measurement techniques applied determine the emittance integrated over the entire bunch length. However, for FEL physics, the emittance of bunch slices much shorter than the bunch length is the relevant parameter. It is likely that, due to spurious dispersion and wakefields, the bunch axis is tilted about a transverse axis such that the projected emittance is larger than the emittance of any slice. Based on these considerations we estimate the normalized slice emittance in the undulator at (6 ± 3) π mrad mm.

A bunch compressor is inserted between the two accelerating modules, in order to increase the peak current of the bunch up to 500 A, corresponding to 0.25 mm bunch length (rms) for a 1 nC bunch with Gaussian density profile. Experimentally, it is routinely verified that a large fraction of the bunch charge is compressed to a length below 0.4 mm (rms) [27]. There are indications that the core is compressed even further. We estimate the peak current for the FEL experiment at (400 ± 200) A.

For radiation intensity measurements we used a PtSi photodiode integrating over all wavelengths. The detector unit was placed 12 m downstream the undulator exit. A 0.5 mm iris was placed in front of the photodiode in order to avoid saturation effects.

In summary, it should be emphasized that full control of the transverse and longitudinal phase space distribution of the electron beam is essential for SASE FEL operation.

Parameters like peak current (i.e. bunch lengths in the 100 μm range) and slice emittance (for slices in the micrometer range) determine the SASE power exponentially. Thus, already modest uncertainties in the knowledge of these parameters can change the undulator length that is required to achieve FEL saturation by a factor of two or so. In particular in view of X-ray FELs, these requirements put new challenges to electron beam diagnostics.

3 FEL MEASUREMENTS

A strong evidence for the FEL process is a large increase in the on-axis radiation intensity if the electron beam is injected such that it overlaps with the radiation during the entire passage through the undulator. The observed intensity inside a window of ± 200 μm around the optimum beam position was enhanced by a factor of more than 100 compared to the intensity of spontaneous radiation observed outside this window.

SASE gain is expected to depend on the bunch charge in an extremely nonlinear way. Fig. 2 shows the measured intensity on axis as a function of bunch charge Q, while the beam orbit is kept constant for optimum gain. The solid line indicates the intensity of the spontaneous undulator radiation multiplied by a factor of 100. The strongly nonlinear increase of the intensity as a function of bunch charge is a definite proof of FEL action. The gain does not further increase if the bunch charge exceeds some 0.6 nC. This needs further study, but it is known that the beam emittance becomes larger for increasing Q thus reducing the FEL gain.

A typical wavelength spectrum of the radiation at TTF FEL (taken on axis at maximum FEL gain) is presented in Fig. 3. The central wavelength of 108.5 nm is consistent with the measured beam energy of (233±5) MeV and the known undulator parameter K=1.17, see Eq. (1). Similar spectra have been measured at wavelengths between 80 nm and 180 nm by properly tuning the electron energy. The intensity gain determined with the CCD camera of the spectrometer is in agreement with the photodiode result.

A characteristic feature of SASE FELs is the concentration of radiation power into a cone much narrower than that of wavelength integrated undulator radiation, whose opening angle is in the order of of 1/γ. Measurements done by moving the 0.5 mm iris horizontally together with the photo diode confirm this expectation, see Fig. 4. To be visible on this scale, the spontaneous intensity is amplified by a factor of 30. The energy flux is 2 nJ/mm^2 at the location of the detector and the on-axis flux per unit solid angle is about 0.3 J/sr (assuming a source position at the end of the undulator). This value was used as a reference point for the numerical simulation of the SASA FEL with the code
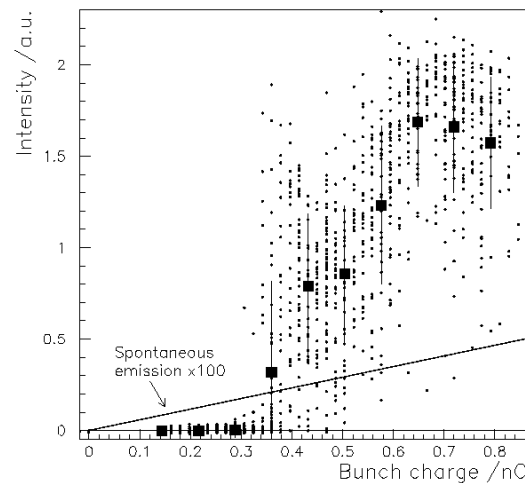
Figure 2: SASE intensity versus bunch charge measured at TTF FEL. The straight line is the spontaneous intensity multiplied by a factor of 100. To guide the eye, mean values of the radiation intensity are shown for some bunch charges (dots). The vertical error bars indicate the standard deviation of intensity fluctuations, which are due to the statistical character of the SASE process, see Eq. (3).

FAST [28]. The longitudinal profile of the bunch current was assumed to be Gaussian with an rms length of 0.25 mm. The transverse distribution of the beam current density was also taken to be Gaussian. Calculations have been performed for a Gaussian energy spread of 0.1%, and the normalized emittance ε_n was varied in the simulations between 2 and 10 π mrad mm . Our calculations show that in this range of parameters the value of the effective power of shot noise P_{in} and coupliing factor A ~0.1 (see eq. 2) are nearly constant. A level of energy flux of 0.3 J/sr is obtained at five field gain lengths L_g. With these parameters the FEL gain can be estimated at G ≈ 3×10^3 with a factor of 3 uncertainty which is mainly due to the imprecise knowledge of the longitudinal beam profile. If we assume that the entire undulator contributes to the FEL amplification process, we estimate the normalized emittance ε_n at 8 π mrad mm in reasonable agreement with the measurements. Figs. 3 and 4 include typical theoretical spectral and angular distributions as calculated by our numerical simulation. In both cases the experiment curves are wider than the simulation results. A possible source of widening is energy and orbit jitter, since the experimental curves are results of averaging over many bunches. This is confirmed by more recent measurements taken at improved energy stability, where the agreement with theory is much better. Large SASE gain was achieved in a stable and reproducible way for several weeks.

Similarly, a SASE gain as high as G = 3×10^5 was demonstrated 1998 at Los Alamos at 12 μm wavelength [13], and the LEUTL experiment achieved a gain above 10^2 at 530 nm wavelength [14].
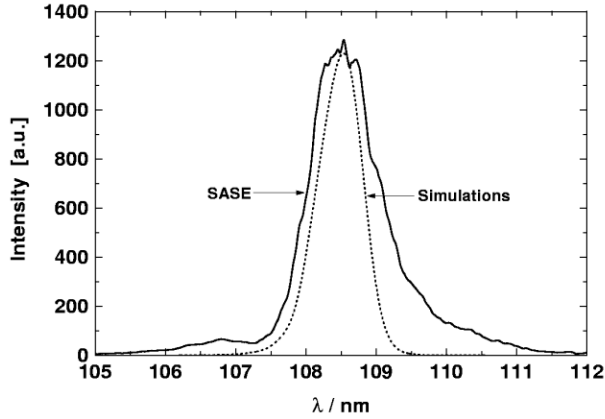
Figure 4: Wavelength spectrum of the central radiation cone (collimation angle ±0.2 mrad), taken at maximum gain at the TTF FEL at DESY. The dotted line is the result of numerical simulation. The bunch charge is 1 nC.
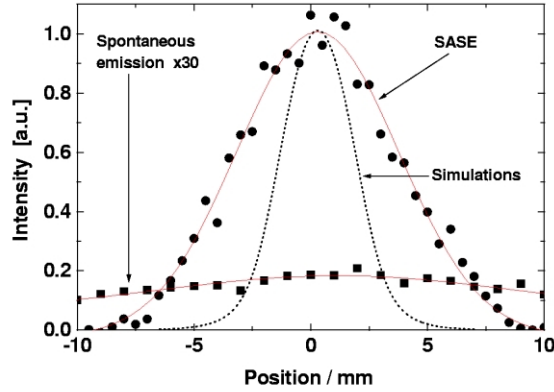
Fig. 5: Horizontal intensity profile of SASE FEL and spontaneous undulator radiation (x30), measured with a photodiode behind a 0.5 mm aperture in a distance of 12 m from the end of the undulator. The dotted line is the result of numerical simulation.

It is essential to realize that the fluctuations seen in Figs. 2 and 3 are not primarily due to unstable operation of the accelerator but are inherent to the SASE process. Shot noise in the electron beam causes fluctuations of the beam density, which are random in time and space [29]. As a result, the radiation produced by such a beam has random amplitudes and phases in time and space and can be described in terms of statistical optics. In the linear regime of a SASE FEL, the radiation pulse energy measured in a narrow central cone (opening angle ±20 μrad in our case) at maximum gain is expected to fluctuate according to a gamma distribution $p(E)$ [30],

$$p(E) = \frac{M^M}{\Gamma(M)} \left(\frac{E}{\langle E \rangle} \right)^{M-1} \frac{1}{\langle E \rangle} \exp \left(-M \frac{E}{\langle E \rangle} \right) \quad (3)$$

where $\langle E \rangle$ is the mean energy, $\Gamma(M)$ is the gamma function with argument M, and $M^{-1} = \langle (E-\langle E \rangle)^2 \rangle / \langle E \rangle^2$ is the normalized variance of E. M corresponds to the number of longitudinal optical modes. Note that the same kind of statistics applies for completely chaotic polarized light, in particular for spontaneous undulator radiation.

For these statistical measurements the signals from 3000 TTF FEL radiation pulses have been recorded, with the small iris (0.5 mm diameter) in front of the photo diode to guarantee that transversely coherent radiation pulses are selected. As one can see from Fig. 5, the distribution of the energy in the radiation pulses is quite close to the gamma distribution. The relative rms fluctuations are about 26% corresponding to $M = 14.4$. One should take into account that these fluctuations arise not only from the shot noise in the electron beam, but the pulse-to-pulse variations of the beam parameters can also contribute to the fluctuations. Thus, the value $M \approx 14$ can be considered a lower limit for the number of longitudinal modes in the radiation pulse. Using the width of radiation spectrum we calculate the coherence time [30] and find that the part of the electron bunch contributing to the SASE process is at least 100 μm long. From the quality of the fit with the gamma distribution we can also conclude that the statistical properties of the radiation are described with Gaussian statistics. In particular, this means that there are no FEL saturation effects.
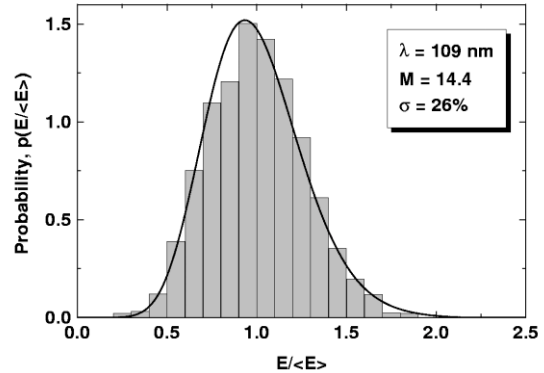
Fig. 6: Probability distribution of SASE intensity. The rms fluctuation yields a number of longitudinal modes M = 14. The solid curve is the gamma distribution for M = 14.4. The bunch charge is 1 nC.

4 SUMMARY

Powerful SASE has become an unquestionable reality in the IR, visible and VUV wavelength regime, and reliable operation was demonstrated at DESY over several weeks. To date, all observations are in agreement with the present SASE FEL models, so optimism is justified that even shorter wavelengths will be reached in close future. It

should be clear, on the other hand, that for X-ray user facilities there is still a way to go: The SASE gain demonstrated so far is still some orders of magnitude below FEL saturation. Also, stable operation with long pulse trains containing several thousand pulses and flexible timing pattern, as requested by users, will remain a challenge for accelerator physicists for a while.

REFERENCES

[1] J.M. Madey, *J. Appl. Phys.* **42** 1906 (1971)

[2] W.B. Colson, *Nucl. Instr. and Meth.* **A429** 37-40 (1999)

[3] K.J. Kim, *Phys. Rev. Lett.* **57** 1871 (1986)

[4] S. Krinsky, L.H. Yu, *Phys. Rev.* **A35** 3406 (1987)

[5] E.L. Saldin, E.A. Schneidmiller, M.V. Yurkov, "The Physics of Free Electron Lasers", Springer (1999) and references therein

[6] A.M. Kondratenko, E.L. Saldin, *Part. Accelerators* **10**, 207 (1980)

[7] R. Bonifacio, C. Pellegrini, L.M. Narducci, *Opt. Commun.* **50** 373 (1984)

[8] H. Winick, et al., *Proc. PAC Washington* and SLAC-PUB-6185 (1993)

[9] R. Brinkmann, et al., *Nucl. Instr. and Meth.* **A 393** 86-92 (1997)

[10] R. Brinkmann, G. Materlik, J. Rossbach, A. Wagner (eds.), DESY 1997-048 and ECFA 1997-182 (1997)

[11] H.-D. Nuhn, J. Rossbach, *Synchrotron Radiation News* Vol. 13, No. 1, 18 – 32 (2000)

[12] D. E. Moncton, *Proc. Linac Conf.*, 1048, Argonne (1999)

[13] M. Hogan, et al., *Phys. Rev. Lett.* **81** 4867 (1998)

[14] S.V. Milton et al., "Observation of Self-Amplified Spontaneous Emission and Exponential Growth at 530 nm" submitted to *Phys. Rev. Lett.* (2000)

[15] J. Andruszkow et al., "First Observation of Self-Amplified Spontaneous Emission in a Free-Electron Laser at 109 nm Wavelength", submitted to *Phys. Rev. Lett.* (2000)

[16] W. Brefeld, et al., *Nucl. Instr. and Meth.* **A393** 119-124 (1997)

[17] T. Åberg, et al., A VUV FEL at the TESLA Test Facility at DESY, Conceptual Design Report, DESY Print TESLA-FEL 95-03 (1995)

[18] J. Rossbach, *Nucl. Instr. and Meth.* **A 375** 269 (1996)

[19] J.-P. Carneiro, et al., *Proc. 1999 Part. Acc. Conf.,* New York 2027-2029 (1999)

[20] P. Michelato, et al., *Nucl. Instr. Meth.* **A445**, 422 (2000)

[21] I. Will, S. Schreiber, A. Liero, W. Sandner, *Nucl. Instr. Meth.* **A445**, 427 (2000)

[22] H. Weise, *Proc. 1998 Linac Conf.* Chicago, 674-678 (1998)

[23] Y. M. Nikitina, J. Pflüger, *Nucl. Instr. and Methods* **A375** 325 (1996)

[24] U. Hahn, J. Pflüger, G. Schmidt, *Nucl. Instr. and Methods* **A429** 276 (1999)

[24] U. Hahn, et al., *Nucl. Instr. Meth.* **A445**, 442 (2000)

[25] J. Pflüger, *Nucl. Instr. Meth.* **A445**, 366 (2000)

[26] H. Edwards, et al., *Proc. 1999 FEL Conf*, Hamburg, to be published in *Nucl. Instr. and Meth. A* (2000)

[27] M. Geitz, G. Schmidt, P. Schmüser, G. v. Walter, *Nucl. Instr. Meth.* **A445**, 343 (2000)

[28] E. L. Saldin, E. A. Schneidmiller, M. V. Yurkov, *Nucl. Instr. and Meth.* **A 429** 233 (1999)

[29] R. Bonifacio, et al., *Phys. Rev. Lett.* **73** 70 (1994)

[30] E. L. Saldin, E. A. Schneidmiller, M. V. Yurkov, *Opt. Commun.* **148** 383 (1998)

Table 1: Typical parameters of recent SASE FEL experiments.

Parameter	Unit	UCLA/LANL [13]	LEUTL [14]	TTF FEL [15]
beam energy at undulator	MeV	18	217	233 ± 5
rms energy spread	MeV	0.045	0.2	0.3 ± 0.2
rms transverse beam size	μm	115-145	130	100 ± 30
ε_n (normalized emittance) in the undulator	π mrad mm	?	5	6 ± 3
electron bunch charge	nC	2	0.7	1
peak electron current	A	170	150	400 ± 200
bunch spacing	ns	9.23	0.35	1000
repetition rate	Hz	1	10	1
λ_u (undulator period)	mm	20.5	33	27.3
undulator peak field	T	0.54	1.006	0.46
effective undulator length	m	2.0	12	13.5
λ_{ph} (radiation wavelength)	nm	12000	530	109
FEL gain		$3 \cdot 10^5$	$> 1 \cdot 10^2$	$3 \cdot 10^3$
FEL radiation pulse length FWHM	ps	6	5	0.3 - 1